

Entropy Collapse in Mobile Sensors: The Hidden Risks of Sensor-Based Security

Carlton Shepherd^[0000-0002-7366-9034] and Elliot A. J. Hurley

School of Computing
Newcastle University
Newcastle-upon-Tyne, UK
{carlton.shepherd,e.a.j.hurley2}@ncl.ac.uk

Abstract. Mobile sensor data has been proposed for security-critical applications such as device pairing, proximity detection, and continuous authentication. However, the foundational assumption that these signals provide sufficient entropy remains under-explored. In this work, we systematically analyse the entropy of mobile sensor data across four diverse datasets spanning multiple application contexts. Our findings reveal pervasive biases, with single-sensor mean min-entropy values ranging from 3.408–4.483 bits ($\sigma=1.018-1.574$) despite Shannon entropy being several multiples higher. We further demonstrate that correlations between sensor modalities reduce the worst-case entropy of using multiple sensors by up to $\approx 75\%$ compared to average-case Shannon entropy. This brings joint min-entropy well below 10 bits in many cases and, in the best case, yielding only ≈ 24 bits of min-entropy when combining 20 sensor modalities. These results call into question the widely held assumption that adding more sensors inherently yields higher security. We ultimately caution against relying on raw sensor data as a primary source of randomness.

Keywords: Entropy · Sensors · Mobile security

1 Introduction

Modern mobile devices come equipped with an array of embedded sensors—accelerometers, gyroscopes, magnetometers, and others—that capture continuous motion and environmental data at fine temporal granularity. This rich sensor data has enabled applications from activity recognition to context-aware computing. More recently, research has proposed leveraging these signals for security-critical tasks such as cryptographic key generation, zero-interaction device pairing, and continuous authentication. A crucial yet under-explored assumption underpins such designs: sensor data provides sufficient unpredictability to thwart adversarial inference. Traditional “shake-to-pair” protocols [1] rely on motion patterns to establish secure communication between co-located devices, while newer techniques incorporate ambient phenomena—characteristics of magnetic fields [2] and thermal fluctuations [3]—to mitigate relay attacks or reduce user-driven authentication prompts. Despite these advancements, fundamental questions remain. Multi-modal sensing is often advocated to counter

sensor-specific weaknesses [2, 4–6], but the quantitative security benefits of combining multiple sensors have not been rigorously evaluated. Many existing studies rely on heuristic assessments or machine learning classifiers, e.g. [2, 4–7], that do not address core cryptographic requirements: how much entropy do sensors truly provide, and whether multi-modal combinations yield proportional security gains or suffer from inter-sensor correlations.

Our analysis reveals systemic limitations. Commodity sensors exhibit significant biases, with gyroscopes yielding min-entropy as low as 0.96 bits—well below cryptographic thresholds. Although multi-modal sensor fusion mitigates some of these issues, non-uniform distributions and inter-sensor correlations reduce the worst-case min-entropy by $\approx 40\text{--}75\%$ compared to average-case Shannon entropy. These findings challenge the notion that increasing the number of sensors automatically strengthens security, and underscore the inadequacy of raw sensor data as a reliable entropy source. Our contributions are:

- We introduce the first systematic approach to evaluating sensor entropy across diverse modalities and datasets using various entropy metrics (max, Shannon, collision, and min-entropy).
- We empirically demonstrate how inter-sensor correlations and biases erode entropy, casting doubt on the proposition that using multiple sensors adds substantially to security.
- Ultimately, we advise against relying on commodity sensors as primary sources of randomness for security-critical applications, both on a single- and multiple-sensor basis.

The rest of this paper is organised as follows: §2 discusses sensor-based security mechanisms and established entropy metrics. §3 explains our experiment design for entropy estimation, including the threat model and dataset selection. §4 presents empirical results of our analyses and §5 discusses the implications for system design. We conclude in §6 with recommendations for further work. Our analysis framework is made publicly available to foster future research.¹

2 Background

This section discusses sensor-based applications primitives, critiques existing approaches, and formalises the entropy metrics underpinning our analysis.

2.1 Mobile Sensor-based Security Applications

One major security application of mobile sensors is proximity detection, particularly for mitigating man-in-the-middle and relay attacks on mobile devices [4, 6–8]. Mehrnezhad et al. [6] introduced a technique that uses accelerometer readings to verify that an NFC payment instrument and terminal are physically tapped together. The authors posit that “*physical tapping causes random but correlated*

¹ <https://github.com/cgshep/entropy-collapse-mobile-sensors>

vibrations at both devices, which are hard to forge (or reproduce)” (p.1, [6]). The work reports an equal error rate (EER) of 17.65% using a machine learning-based approach. Gurulian et al. [7] also explored the use of shared vibration patterns between users using unique vibration patterns generated by one device. Mobile sensors have also found utility in tackling the longstanding problem of continuous authentication [9–16], where sensor data is used to authenticate users passively without explicit interaction. (with up to 99% classification accuracy in some instances [10]). Mobile sensors have also been proposed as enabling novel device pairing schemes for secure communication, e.g. [1, 17].

The notion of ‘hardness’ is typically inferred based on a machine learning-based analysis; it is not grounded in standard quantitative methods used in the field of authentication, such as Shannon [18] and min-entropy [19]. A general approach to follows one of those given by Shrestha et al. [20]. Here, sensor data is collected from N users from which various features are extracted in the time or frequency domain (e.g. cross-correlation, spectral energy, Hamming, Euclidean and mean-absolute distances) [4, 6]. Calculating false positive (FPR) and negative (FNR) rates [1], precision and recall [12], EERs [6, 7], Receiver-Operator Curves (ROC) [16], and accuracy [16] have been used to evaluate the effectiveness of distinguishing between legitimate and illegitimate samples. User studies have also been employed to evaluate the effectiveness of sensor-based authentication systems [1, 11]. However, machine learning-based evaluation metrics do not measure intrinsic entropy—a crucial factor in determining whether sensor data is a suitable source of randomness for security applications. Some work has attempted to assess the entropy of sensor signals, but this represents a minority. T2Pair by Li et al. [21] 32.3–38.5 bits of Shannon entropy, with a refinement by Wu et al. [22] reporting 51–54 bits of Shannon entropy. Even in the best cases, this is low relative to modern cryptographic standards.

We point to adjacent work that has questioned the utility of mobile sensors. Markantonakis et al. [4], building on Gurulian et al. [23] and Shepherd et al. [24], presented a reproducibility study disputing the claimed effectiveness of mobile sensors when deployed under real-world time constraints. Using consumer off-the-shelf devices, the work reports that sensors available through the Android platform could not be used to reliably detect man-in-the-middle attacks in NFC contactless transactions within the 500ms time window required by the EMV payment protocol. Under those constraints, the effectiveness drastically decreased compared to previously reported results. Indeed, it was lower to the extent such that sensors could not be recommended for mobile transactions without posing significant usability and security issues in practice.

2.2 Sensor Entropy Analyses

In earlier work, Voris et al. [19] investigated the use of accelerometers as true random number generators (TRNGs), specifically aboard a WISP RFID tag and a Nokia N97 mobile phone. The authors find that min-entropy—defined in §2.3—that min-entropy is proportional to the motion applied to the device, and that

stationary movement has the lowest min-entropy. Intrinsic noise from the sensor’s circuitry and seismic noise, and the sampling rate of its analog-to-digital converter (ADC) are considered other significant influences on the generated entropy. Min-entropy values of 3.1–11.4 bits were measured depending on the movement of the accelerometer. Lv et al. [25] analyse three mobile sensors on an undisclosed Xiaomi Redmi smartphone: a triaxial accelerometer, gyroscope, and magnetometer. Min-entropy values of 0.593–5.876 are reported, depending on the modality and the entropy estimation method used. Krhovják et al. [3] examine the entropy of image and audio data collected from mobile phone cameras and microphones respectively. Using Nokia N73 and E-Ten X500 and M700 phones, Shannon entropy values of 2.9 (microphone) and 2.408–5.376 (camera) are reported, with min-entropy of 0.5 (microphone) and 0.754–3.928 (camera). Hennebert et al. [26] present an analysis of 10 sensor modalities available on two wireless sensor monitors: a TI eZ430-RF2500 and a Zolertia Z1. The work uses a single-sensor analysis, presenting min-entropy values between 0–7.85. Motion sensors, e.g. accelerometer and vibration sensors, yielded the highest entropy.

Mobile sensors have also been proposed as entropy sources in low-cost RNG designs. Suciú et al. [27] propose using a phone’s GPS module along with its accelerometer, gyroscope and orientation sensors. Using data from an HTC Google Nexus One, the approach passes the tests established in the NIST SP 800-22 [28] suite, but no precise entropy values are presented. Wallace et al. [29] explore the use of accelerometer, gyroscope, microphone, WiFi, GPS and camera data as randomness sources. Mobile sensors are inherently *opportunistic* entropy sources, contrasting with dedicated hardware like ring oscillators, those build on Johnson-Nyquist thermal noise, or quantum-based generators (e.g. see [30]). Mobile sensors depend heavily on user behaviour and environmental, introducing biases and correlations absent in controlled entropy sources. Existing sensor-based security mechanisms largely overlook these dynamics, relying instead on heuristic assessments or those based on machine learning-based evaluation metrics [12, 16]. Such approaches do not account well for skewed distributions and other biases in the underlying data. This contrasts with typical entropy measures used in RNG analyses or in the study of authentication systems [31]. For instance, NIST SP800-90B [32] and AIS 20/31 [33] recommend the use of min-entropy to estimate ‘worst-case’ unpredictability of a given source. Our study bridges the gap by systematically evaluating entropy across modalities and datasets.

2.3 Definitions

We use the following definitions and notation throughout this work.

Definition 1 (Rényi Entropy). *Let X be a discrete random variable taking values in a set \mathcal{X} with probability mass function $p(x)$. The Rényi entropy of order α ($\alpha > 0$, $\alpha \neq 1$) is defined as*

$$H_\alpha(X) = \frac{1}{1-\alpha} \log\left(\sum_{x \in \mathcal{X}} p(x)^\alpha\right). \quad (1)$$

We draw attention to four special cases of α that are widely used in the literature. Firstly, the *Hartley (Max) Entropy* ($\alpha = 0$), given in Eq. 2, is the logarithm of the number of possible outcomes that have non-zero probability; it serves effectively as an upper bound.

$$H_0(X) = \log \left| \{x \in \mathcal{X} : p(x) > 0\} \right|. \quad (2)$$

Second is the *Shannon Entropy* (Eq. 3), which corresponds to the classical definition of entropy in information theory, and is the limit of H_α as $\alpha \rightarrow 1$.

$$H_1(X) = - \sum_{x \in \mathcal{X}} p(x) \log p(x). \quad (3)$$

Another case is the *Collision Entropy* ($\alpha = 2$), quantifying the probability of “collisions” of multiple draws from X . This is given in Eq. 4.

$$H_2(X) = - \log \left(\sum_{x \in \mathcal{X}} p(x)^2 \right). \quad (4)$$

H_1 provides an average-case measure of uncertainty. It takes into account the entire distribution of outcomes; however, an adversary may only need to guess the most likely event to gain an advantage. Min-entropy is thus used as a conservative, worse-case metric, accounting for the least favorable distribution of outcomes. This is the *Min-Entropy* (Eq. 5), i.e. the value at the limit $\alpha \rightarrow \infty$.

$$H_\infty(X) = - \log \left(\max_{x \in \mathcal{X}} p(x) \right). \quad (5)$$

Note that H_α is a non-increasing function of α , i.e. $H_\infty(X) \leq H_2(X) \leq H_1(X) \leq H_0(X)$. $H_\infty(X)$ focuses on the single most likely outcome, providing a strictly tighter (and generally minimum) bound on uncertainty. We observe that min-entropy ensures that even the most skewed probability distributions still meet the required security guarantees; indeed, it is a recommended method for assessing entropy sources in NIST SP800-90B [32] and AIS 20/31 [33]. We also rely on joint entropy for assessing the entropy of multiple random variables.

Definition 2 (Joint Rényi Entropy). Let X_1, X_2, \dots, X_n be discrete random variables that jointly take values in $\mathcal{X}_1 \times \mathcal{X}_2 \times \dots \times \mathcal{X}_n$, with joint probability mass function $p(x_1, x_2, \dots, x_n)$. The Rényi entropy of order α ($\alpha > 0, \alpha \neq 1$) for these n variables is defined as the following, where the sum is taken over all (x_1, \dots, x_n) in $\mathcal{X}_1 \times \mathcal{X}_2 \times \dots \times \mathcal{X}_n$:

$$H_\alpha(X_1, X_2, \dots, X_n) = \frac{1}{1-\alpha} \log \left(\sum_{(x_1, \dots, x_n)} p(x_1, \dots, x_n)^\alpha \right) \quad (6)$$

In the limit $\alpha \rightarrow 1$, then $H_\alpha(X_1, X_2, \dots, X_n)$ converges to the classical joint Shannon entropy of these n variables. To support the later discussion on Chow-Liu trees—our approach to joint entropy estimation—we also define the Kullback-Leibler divergence.

Definition 3 (Kullback-Leibler (KL) Divergence). *Given a true probability distribution $P(x)$ of a random variable and an approximate or reference distribution $Q(x)$, the KL divergence is defined as follows:*

$$D_{KL}(P \parallel Q) = \sum_{x \in \mathcal{X}} P(x) \log \left(\frac{P(x)}{Q(x)} \right) \quad (7)$$

3 Experiment Design

3.1 Threat Model and Assumptions

We consider an adversary whose primary objective is to compromise sensor-based key generation or authentication schemes by exploiting the inherent biases or predictable patterns within sensor data. In particular, we assume the adversary has full or near-full knowledge of the probability distribution of sensor outputs. They may obtain this through statistical modeling of publicly available datasets, prolonged observation of target users, or eavesdropping on sensor data streams.

We exclude adversarial capabilities such as fault-injection attacks or hardware attacks, e.g. see [34]. While such attacks could further reduce the effective entropy space, we regard them as a higher level of sophistication—an important future research direction but not the focus here. Lastly, rather than brute-forcing all possible sensor outputs, we assume a more strategic approach: the adversary uses its knowledge of the sensor’s distribution to prioritise the most probable (or most easily predicted) outcomes. By iterating guesses in order of descending probability, they minimise their expected effort. This threat model represents a realistic adversary who can capitalise on statistical biases in sensor data but does not directly sabotage or physically compromise the device. Our goal is to evaluate whether typical sensor data distributions—even aggregated from diverse users—offer sufficient entropy to resist such knowledge-driven attacks.

3.2 High-level Methodology

We aim to determine the *global* (i.e., population-level) entropy characteristics of various mobile sensors under ordinary usage conditions, rather than focusing on per-user or scenario-specific differences. This choice reflects common real-world deployments, which often must accommodate a wide range of behaviors and environments with minimal tailoring. Our approach involves five main stages:

1. We acquire large-scale sensor readings from publicly available datasets that capture diverse user activities and device usage patterns. These datasets encompass different motion, environmental, and orientation sensors. Detailed descriptions of each dataset are provided at the end of this section.
2. We merge sensor readings into a single, global distribution for each sensor modality in each dataset. For sensors that are inherently discrete or quantised (e.g., integer output ranges), we simply count occurrences. For sensors that

produce (quasi-)continuous values, we rely on quantisation strategies (Freedman–Diaconis binning) to partition the output space and approximate an empirical probability mass function.

3. From these global distributions, we compute max, Shannon and collusion entropies to measure the best- and average-case uncertainties of sensor outputs, along with the min-entropy to characterise the worst-case unpredictability.
4. Many real-world proposals combine multiple sensor streams to purportedly increase security. To assess the impact on worst-case unpredictability, we use Chow-Liu trees to approximate the joint distributions of different sensor modalities. This allows us to estimate higher-dimensional entropies without incurring prohibitive computational costs. We discuss this in §4.3.
5. Finally, we interpret the resulting entropy measures, focusing on whether sensor outputs remain sufficiently unpredictable against an informed adversary. We compare single-sensor versus multi-sensor scenarios to verify if combining modalities truly alleviates biases or simply adds redundant data susceptible to similar predictability concerns.

Throughout this process, we remain mindful of well-documented constraints with NIST SP 800-90B, SP 800-22 [32], and AIS 20/31 [33] in analysing multi-sensor data streams [25, 35]. Such frameworks were not designed to analyse the joint entropy of complex, multivariate data sources, which is the aim of this work. (For example, NIST SP 800-90B focusses on assessing univariate entropy sources with reduced, i.e. 8-bit, output sizes [32, 35]). To begin with, we sought publicly available sensor datasets suitable for analysing motion and environmental data at scale. Our search involved broad queries across IEEE DataPort, Google Scholar, Google Dataset Search, and GitHub. Several ostensibly “open” datasets either were no longer downloadable or imposed restrictive licensing terms [36–38]. Ultimately, we narrowed our scope to four datasets that offer diverse usage contexts, consistent sampling rates, and documented sensor modalities:

- *UCI-HAR* [39]: A widely referenced dataset for human activity recognition, comprising smartphone sensor recordings from multiple subjects performing daily activities. Data includes triaxial accelerometer and gyroscope signals.
- *University of Sussex–Huawei Locomotion (SHL)* [40, 41]: sampled at 100 Hz. Multiple Huawei Mate 9 phones attached across the users’ body in a body area network (BAN). The publicly available SHL Preview dataset is used, comprising three recording-days per user (a total of 59 hours of data). To scope this study, we use the motion sensors dataset from the handheld mobile phone as a good fit with related work (see §2).
- *Relay* [23]: Contains sensor measurements for approximately 1,500 NFC-based contactless transactions, each recorded at 100 Hz across several physical locations (e.g., cafés). The dataset encompasses accelerometer, gyroscope, and environmental readings taken in realistic payment scenarios.
- *PerilZIS* [42]: Collected at 10 Hz from a Texas Instruments SensorTag, a Samsung Galaxy S6, and a Samsung Galaxy Gear, this dataset spans multiple zero-interaction security use cases in an office environment.

These four datasets provide a variety of sensor types, user activities, and sampling rates, allowing us to explore how intrinsic biases and correlations manifest across different real-world scenarios. Next, we detail how we preprocess and aggregate this data to form global distributions for our entropy analyses.

4 Entropy Analysis

In this section, we analyze the intrinsic entropy of sensor data under the threat model described in §3. We begin by discussing the challenges in quantising naturally continuous sensor values for discrete-entropy calculations, then present our single-sensor findings. Later sections examine multi-sensor joint entropies and the complexities of sensor fusion.

4.1 Pre-processing

A crucial, yet underexplored, issue in prior work (e.g. [19, 25, 26, 31]) is how to convert inherently continuous sensor outputs into suitable discrete values for entropy estimation. For example, Shannon entropy and min-entropy, as defined in Eqs. 3 and 5, rely on discrete random variables. Physical quantities such as linear acceleration or angular velocity are continuous in nature, even though modern sensors employ internal analog-to-digital conversion with a finite resolution. However, a sensor’s advertised resolution (e.g. 12 bits for the widely used Bosch BMA mobile accelerometer [43]) does *not* imply uniform or truly high-fidelity coverage across its range. Everyday usage introduces biases and clustering, resulting in some measurements occurring far more frequently than others. For instance, *UCI-HAR* data shows accelerometer readings widely spread in certain axes, while approximately 60% of gyroscope readings hover near zero (see Figure 2). Such heavy skew or near-constant values radically diminish real-world entropy, which would otherwise benefit from uniformly distributed values.

Beyond skew and bias, another practical challenge arises when extremely fine-grained values appear only infrequently or are negligible in real usage contexts. Treating every minute fluctuation (e.g. $9.000001ms^{-2}$ vs. $9.000002ms^{-2}$ for an accelerometer) as distinct outcomes can artificially inflate entropy estimates, while providing no real-world unpredictability advantage. Indeed, in real-world applications, it is the ‘similarity’ of measurements that is considered useful in related proposals, e.g. based on machine learning. It would be extremely difficult for users to reliably reproduce high-precision movements capable of effectively utilising a sensor’s digital resolution (say at $0.00001ms^{-2}$ for an accelerometer). To address this, we discretise the data values into bins of similar value. However, this raises a further question of what constitutes a good strategy for selecting the number of bins and their widths? Several techniques exist that make assumptions about the underlying distribution, e.g. Gaussian; have different computational complexities; and are robust to outliers and data variability. To this end, we use the Freedman-Diaconis method (Eq. 8), a commonly used robust estimator that accounts for data size and its variability. This approach balances capturing

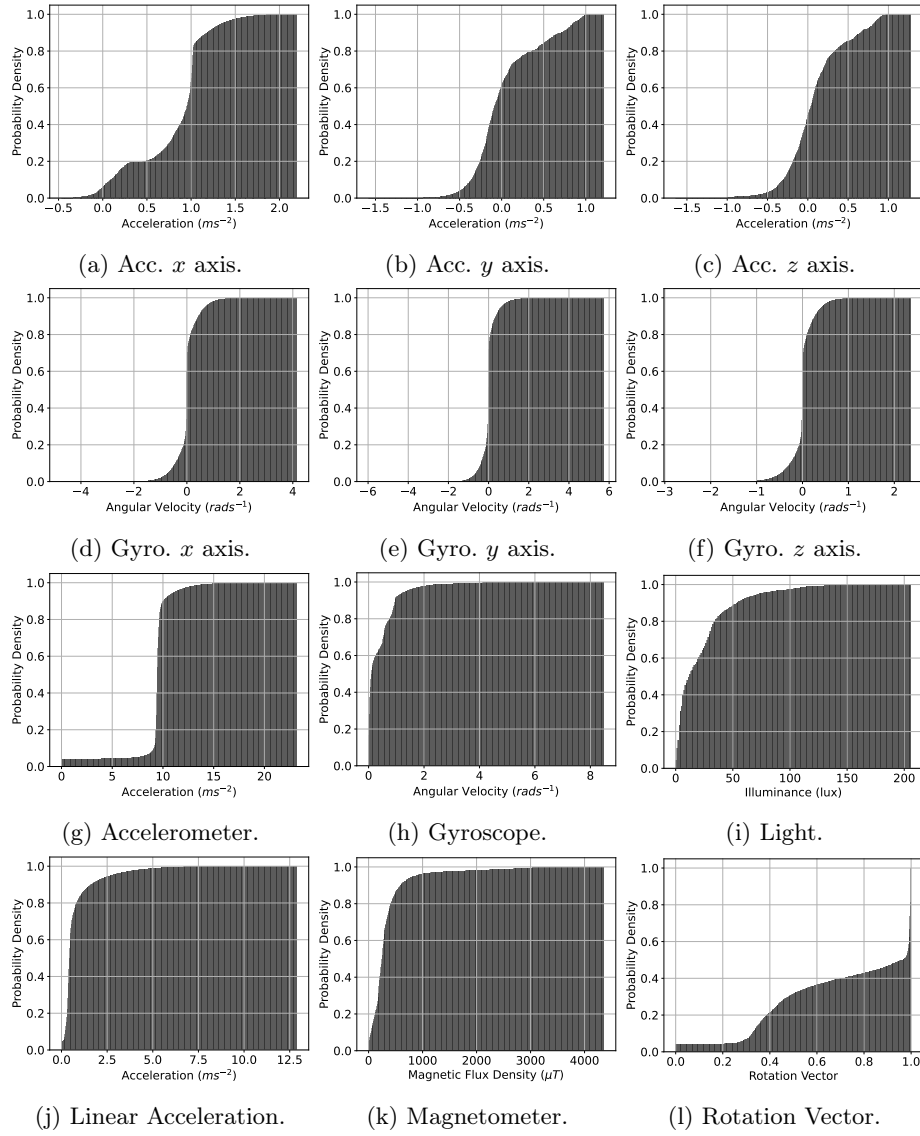


Fig. 1: Global sensor data CDFs – UCI-HAR (a–f) and Relay (g–l) datasets.

sufficient detail with avoiding hyperfine, user-driven distinctions that are outside the scope of this paper.² This is calculated in Eq. 8, where $IQR(x)$ represents the interquartile range of x and n is the total number of samples.

² Alternatively, a binning strategy could be employed that reflects how precisely humans can realistically replicate sensor-input changes. We defer this to future research.

$$h = 2 \cdot \frac{IQR(x)}{n^{1/3}} \quad (8)$$

4.2 Single Sensors

Given the biases discussed above, it is unsurprising that some sensor readings exhibit high predictability in the worst-case sense. We illustrate this by calculating individual-sensor entropy across multiple datasets, splitting multi-dimensional readings (e.g., triaxial accelerometer or gyroscope) into separate axes following Voris et al. [19]. The results are given in Table 1. We note that in the Relay dataset, the data for individual x , y and z components are not given for the accelerometer, gyroscope, and magnetometer sensors. Rather, the authors preprocess triaxial data into its vector magnitude, i.e. $\mathbf{v} = \sqrt{x^2 + y^2 + z^2}$. We give this as “X.Mag” for a given sensor X. For completeness, we compute the magnitude ourselves for other datasets, where applicable, and report the entropy values for this abstract sensor modality.

Several clear patterns emerge from Table 1. Some sensors (e.g. certain accelerometer axes in *SHL* or *PerilZIS*) exhibit moderate min-entropies (4–6 bits). Other sensors, particularly gyroscope axes, (see *UCI-HAR*), show values below 3 bits, indicating high predictability in their most frequent readings. Shannon entropy values (H_1) can be fairly high (up to 10 bits in some cases), whereas min-entropy (H_∞) is often much lower. This gap reflects distributions where a few outcomes dominate, thereby driving worst-case unpredictability down even if the average-case picture is more favorable. Overall, the results confirm that data from individual sensors do not provide sufficient min-entropy for robust security on their own. In the next section, we examine whether combining multiple modalities can meaningfully increase this worst-case unpredictability or whether correlated biases persist across different sensor streams.

4.3 Multi-modal Sensors

Many sensor-based security proposals [2, 4–6, 20] assert that combining multiple sensor modalities can bolster security, based on the intuition that an adversary must accurately predict several data streams, rather than just one. A naïve model assumes each sensor is statistically independent, yielding the simplified relation $H(X_1, X_2, \dots, X_n) = \sum_{i=1}^n H(X_i)$. However, real-world sensor outputs often exhibit significant interdependence. For example, *linear acceleration*, *rotation vector*, and *gravity* in the Android ecosystem are often derived from the same underlying motion sensors, causing strong correlations. Figure 2 illustrates the correlation matrices of the sensors we examine across our four datasets, revealing that many modalities are far from independent.

Complexity challenges. Unfortunately, directly estimating the joint entropy of discrete sensor data often becomes computationally infeasible as the number of

Table 1: Single-sensor entropy values (in bits) for each dataset. Grey cells denote unavailable data for that modality and dataset.

Sensor	Dataset															
	UCI-HAR				SHL				Relay*				PerilZIS			
	H_0	H_1	H_2	H_∞	H_0	H_1	H_2	H_∞	H_0	H_1	H_2	H_∞	H_0	H_1	H_2	H_∞
Acc.X	8.488	7.080	5.876	3.729	11.557	8.732	7.487	4.543					13.012	9.292	6.359	3.626
Acc.Y	8.243	7.231	6.847	5.694	11.425	8.928	7.717	4.500					9.549	5.873	4.483	2.889
Acc.Z	8.455	7.397	7.069	6.020	10.428	7.627	6.366	3.785					9.817	6.671	5.403	4.002
Acc.Mag	8.895	6.284	4.819	3.489	14.583	10.136	8.710	6.435	10.145	6.843	5.808	4.538	13.328	8.273	7.115	4.526
Gyro.X	8.683	5.430	3.504	1.929	15.024	10.532	8.107	4.993					14.528	7.231	4.454	2.805
Gyro.Y	8.439	5.023	3.461	2.300	15.085	10.283	7.601	4.827					14.078	6.715	4.039	2.529
Gyro.Z	8.714	5.675	3.948	2.363	15.281	10.070	5.708	3.083					13.961	6.463	3.836	2.434
Gyro.Mag	8.414	5.759	4.130	2.537	12.123	7.816	5.728	3.699	7.954	4.751	3.442	2.083	14.166	5.565	1.932	0.969
Mag.X					12.845	8.840	8.386	6.374					10.767	7.639	6.816	4.883
Mag.Y					12.263	8.737	8.314	6.223					10.179	7.622	6.605	4.405
Mag.Z					12.516	8.586	8.217	6.228					10.129	7.507	6.726	4.448
Mag.Mag					13.558	9.436	8.771	7.148	7.972	6.147	5.617	4.254	10.293	7.329	6.489	4.454
Rot. Vec.					8.725	7.721	5.970	3.220	5.000	3.307	1.965	1.021				
Grav.X					9.014	8.482	7.266	4.299								
Grav.Y					9.338	8.770	7.602	4.453								
Grav.Z					8.180	7.193	5.418	3.036								
Grav.Mag					14.373	7.988	7.227	6.242	7.794	6.325	5.864	4.532				
LinAcc.X					15.260	10.077	7.621	5.116								
LinAcc.Y					14.859	10.116	7.639	5.224								
LinAcc.Z					14.377	9.951	7.605	4.543								
LinAcc.Mag					12.777	7.968	5.752	3.420	9.175	6.385	5.424	4.222				
Light									7.200	5.331	4.507	3.206	12.152	7.940	7.137	4.552
Humidity													7.943	7.048	6.774	5.546
Temp.					7.295	4.753	2.611	1.332					8.484	7.416	6.941	5.449
Pressure					9.461	8.170	7.723	6.237					8.044	7.006	6.370	5.073
Mean	8.541	6.235	4.957	3.508	13.188	9.266	7.178	4.483	7.891	5.584	4.661	3.408	11.277	7.224	5.717	3.912
S.D.	0.207	0.904	1.461	1.574	1.993	1.148	1.115	1.018	1.612	1.227	1.474	1.379	2.312	0.900	1.526	1.266

*: The authors preprocess triaxial data into its vector magnitude.

modalities increases, due to the curse of dimensionality. Specifically, for n modalities, where each modality X_i is discretised into b_i bins (with $\{b_1, b_2, \dots, b_n\} \subseteq B$), the total number of joint bins scales as $\prod_{i=1}^n b_i$. Applying Freedman–Diaconis binning rules typically results in thousands of bins per modality, causing the number of joint bins to explode combinatorially. Consequently, computing a full joint entropy estimation, as in Eq. 6, becomes intractable. Another concern is the combinatorial explosion of sensor combinations. Let us assume that one has 19 modalities, as in Table 1, then the total number of combinations to analyse is equal to $2^{19} - 20$, skipping single sensors and the empty set. For even moderately large datasets, iterating over every sensor subset and computing its full joint entropy is prohibitively expensive. Addressing these problems is challenging. One mitigation is to reduce the number of bins per modality. However, this inevitably risks oversimplifies the distribution and underestimating its joint entropy. Preliminary experiments confirmed joint entropies could be computed directly for $n \leq 3$ modalities with a maximum of 1250 bins and fewer than 150K total samples from the Relay dataset. Further scaling became infeasible. We

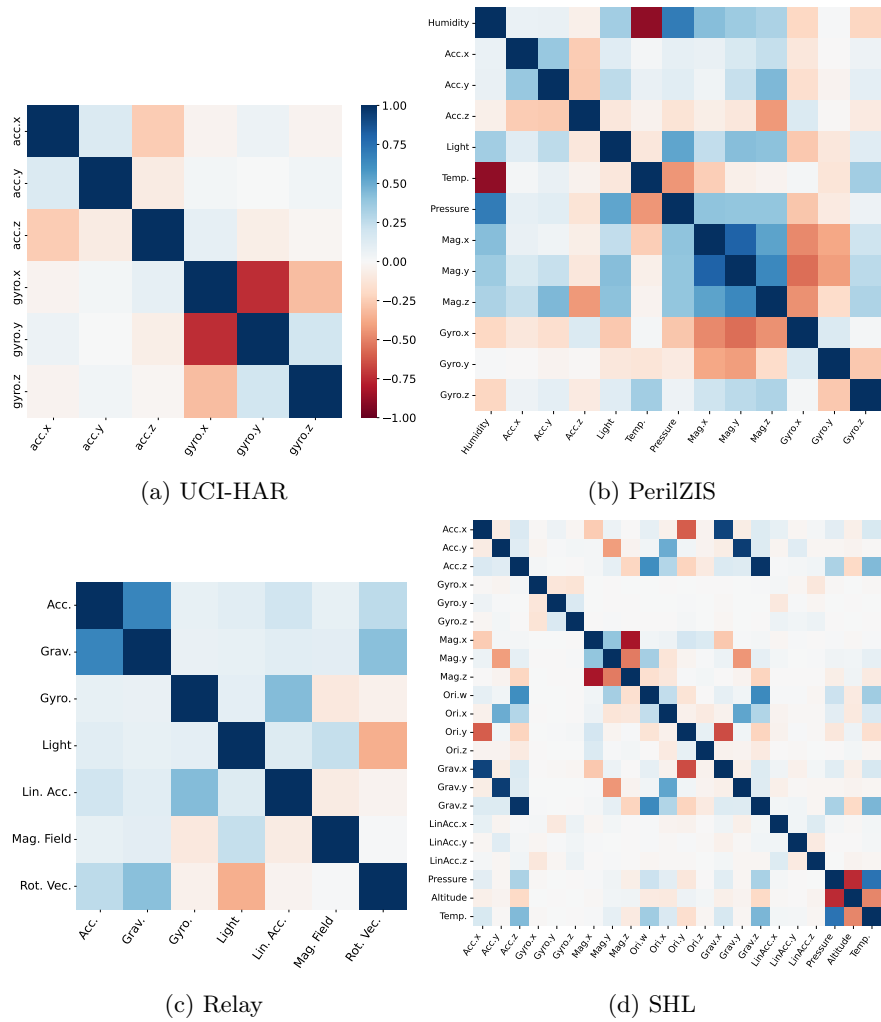


Fig. 2: Sensor correlation matrices for each dataset.

also observed that imposing these smaller bin counts (rather than the thousands implied by Freedman–Diaconis) reduced our single-sensor entropy estimates by approximately 2–3 bits on average compared to those reported in Table 1.

Chow-Liu approximation. To address the problem of high-dimensional entropy estimation, we adopt the Chow-Liu algorithm [44] to approximate the joint probability distribution of multiple sensors using a tree-structured Bayesian network. Specifically, Chow-Liu constructs a maximum-weight spanning tree π over the n modalities, where the edge weights correspond to the mutual information

between pairs of variables. This tree structure minimises the Kullback-Leibler divergence (Def. 2.3) between the true joint distribution and the tree-structured approximation. The joint probability is then estimated as:

$$p_\pi(x_1, \dots, x_n) = p(x_r) \prod_{i \neq r} p(x_i | x_{\pi(x)}) \quad (9)$$

Where $\pi(i)$ denotes the parent of X_i in the tree, and r is the tree’s root node. This model efficiently captures the dominant pairwise dependencies, which is particularly beneficial when exploring the combinatorial relationships of different modalities. The use of Chow-Liu trees was also suggested by Buller and Kaufer [35] for estimating the entropy of multivariate data sources where the range of possible values is high. In our Python implementation, we use the pgmpy [45] library’s TreeSearch module. With the inferred Bayesian network in hand, we can compute the max (H_0), Shannon (H_1), collision (H_2) and min-entropies (H_∞) without resorting to summation over the full exponential state space. Chow–Liu’s acyclic, singly connected structure is crucial: each node has at most one parent, so one can traverse the tree top-down (from root) or bottom-up to accumulate either sums of probabilities (e.g. for collision entropy) or maximum probabilities (e.g. min-entropy). This significantly reduces computation time compared to naïve enumeration.

Our entropy analysis framework systematically evaluates the joint entropy over all valid combinations of sensor modalities. The powerset of the sensor set is generated (with restrictions on minimum and maximum combination lengths) and processed in parallel using Python’s multiprocessing module. Each subset is independently analysed: quantising the data, inferring a Chow–Liu tree, and computing the suite of entropy metrics. Processing all four datasets took approximately 22 hours on our workstation with an Intel i7-6700K (8M cache, 4.20 GHz) and 32 GB RAM on Ubuntu 24.04.

Results. The results are given in Tables 2 to 5, listing the top 10 sensor combinations for each dataset in descending order of min-entropy. The full sensor set consistently achieves the highest entropy values. This behavior is anticipated: adding more modalities increases the theoretical upper bound on entropy (e.g., H_0), and it does not lower the min-entropy. We observe that removing certain modalities often has a negligible impact on worst-case unpredictability. For example, in the SHL dataset (Table 5), while the full sensor suite attains $H_0 = 158.601$ bits and $H_1 = 82.301$ bits, the min-entropy remains at a constant $H_\infty = 21.289$ bits across both the full sensor set and the top-performing subsets. This consistency indicates that, although additional sensors expand the total support (reflected in higher H_0), they do not necessarily enhance worst-case unpredictability (H_∞). Similarly, in Table 3 for the Relay dataset, the combination (Acc., Gyro., Light, Lin. Acc., Mag., Rot. Vec.) achieves $H_\infty = 7.859$ bits, only slightly below the full set’s 8.092 bits. Parallel findings arise in the PerilZIS and SHL datasets, where omitting a small number of sensors from the “All sensors” set has negligible impact on H_∞ . These observations suggest that carefully

chosen sensor subsets can yield nearly optimal min-entropy while reducing the number of modalities and associated overhead (e.g. battery consumption). We provide the full sensor combination results in our open-source repository.

Table 2: Top 10 best-performing sensor combinations (UCI-HAR; in bits).

Modality	H_0	H_1	H_2	H_∞
All sensors	48.061	25.089	17.116	11.008
(Acc.{x,y,z}, Gyro.{y,z})	39.403	22.835	15.999	10.113
(Acc.{x,y,z}, Gyro.{x,y})	39.886	21.456	15.332	9.900
(Acc.{x,y,z}, Gyro.{x,z})	40.222	21.470	15.040	9.411
(Acc.{y,z}, Gyro.{x,y,z})	40.228	21.306	14.698	9.274
(Acc.{x,z}, Gyro.{x,y,z})	40.293	21.260	14.575	9.154
(Acc.{x,y,z}, Gyro.y)	31.228	18.804	13.893	9.065
(Acc.{x,y}, Gyro.{x,y,z})	40.273	21.155	14.208	8.721
(Acc.{x,y,z}, Gyro.z)	31.564	18.775	13.833	8.682
(Acc.{y,z}, Gyro.{y,z})	31.570	18.583	13.400	8.386

Table 3: Top 10 best-performing sensor combinations (Relay; in bits).

Modality	H_0	H_1	H_2	H_∞
All sensors	45.794	25.036	15.725	8.092
(Acc., Gyro., Light, Lin. Acc., Mag., Rot. Vec.)	44.795	24.963	15.334	7.859
(Acc., Grav., Light, Lin. Acc., Mag., Rot. Vec.)	38.385	21.590	14.783	7.702
(Acc., Grav., Gyro., Light, Mag., Rot. Vec.)	37.026	21.001	14.553	7.702
(Grav., Gyro., Light, Lin. Acc., Mag., Rot. Vec.)	36.092	20.794	14.450	7.673
(Acc., Light, Lin. Acc., Mag., Rot. Vec.)	37.385	21.517	14.428	7.469
(Acc., Gyro., Light, Mag., Rot. Vec.)	36.026	20.924	14.270	7.465
(Gyro., Light, Lin. Acc., Mag., Rot. Vec.)	35.092	20.720	14.147	7.439
(Acc., Grav., Gyro., Light, Lin. Acc., Mag.)	41.094	22.794	14.437	7.338
(Acc., Grav., Light, Mag., Rot. Vec.)	29.617	17.555	13.244	7.312

5 Evaluation

This section critically evaluates our sensor entropy findings using existing literature and relevant standards. We then discuss potential mitigations such as randomness extractors, outline inherent limitations of our study and sensor-based approaches, and propose avenues for future enhancements.

5.1 Comparison with Related Work

Prior studies have claimed that mobile sensors can serve as a robust source of security or randomness. Much work has relied on machine-learning-based metrics as a proxy to evaluate such claims [2, 4, 6, 7], with a smaller subset using more

Table 4: Top 10 best-performing sensor combinations (PerilZIS; in bits).

Modalities	H_0	H_1	H_2	H_∞
All sensors	83.662	36.998	33.682	23.926
(Acc.{x,y,z}, Light, Temp., Pres., Mag.{x,y,z}, Gyro.{x,y,z})	76.907	34.258	31.510	23.835
(Acc.{y,z}, Light, Temp., Pres., Mag.{x,y,z}, Gyro.{x,y,z})	72.737	34.246	31.509	23.835
(Acc.{x,z}, Light, Temp., Pres., Mag.{x,y,z}, Gyro.{x,y,z})	72.820	34.243	31.508	23.829
(Acc.{x,y}, Light, Temp., Pres., Mag.{x,y,z}, Gyro.{x,y,z})	72.737	34.229	31.501	22.945
(Acc.{x,y,z}, Light, Temp., Mag.{x,y,z}, Gyro.{x,y,z})	71.384	32.586	30.190	22.945
(Acc.y, Light, Temp., Press., Mag.{x,y,z}, Gyro.{x,y,z})	68.568	34.218	31.500	22.945
(Acc.x, Light, Temp., Pres., Mag.{x,y,z}, Gyro.{x,y,z})	68.650	34.215	31.499	22.945
(Acc.{y,z}, Light, Temp., Mag.{x,y,z}, Gyro.{x,y,z})	67.214	32.575	30.189	22.945
(Acc.{x,y,z}, Light, Temp., Pres., Mag.{x,z}, Gyro.{x,y,z}, Hum.)	76.618	33.816	31.035	21.915

established entropy metrics. Li et al. [21] report 32–38 bits of Shannon entropy for some motion-based secure pairing schemes, and Wu et al. [22] estimate 51–54 bits. However, dedicated entropy analyses frequently demonstrate that *individual* sensors confer very little min-entropy, especially under worst-case assumptions [3, 19, 25, 26]. Our results, derived from a systematic analysis of multiple datasets and modalities (see Tables 2–5), corroborate and challenge these claims.

Single sensors yield low entropy. In line with prior work, we find that min-entropy often remains significantly below the Shannon estimates (e.g., some single-sensor readings yield only 1–3 bits). Our min-entropy estimates often remain significantly lower than their Shannon counterparts (e.g. some single-sensor readings yield only 1–3 bits of min-entropy). This highlights a major gap between average-case unpredictability and worst-case security, which is an important distinction that many earlier evaluations do not fully capture.

Multiple sensors improve worst-case entropy, but not dramatically. While combining more modalities typically raises the upper bound (e.g. Hartley or Shannon entropy), our experiments reveal that min-entropy gains are far smaller than one might hope. In some cases, H_∞ plateaus, indicating that a few highly probable outcomes still dominate the distribution.

Overall, our findings place stricter bounds on the real benefits of mobile-sensor-based approaches. While sensor data can be effective for *classification-based* tasks such as continuous authentication, where strong assurances are not necessarily required, or simple proximity checks, the suitability of sensor data as an attack-resistant random source remains doubtful unless carefully engineered and rigorously evaluated. Min-entropy is critical in scenarios where an adversary can guess the most likely states first; our analysis does not even incorporate adversarial perturbations, meaning real-world attacks could degrade unpredictability even further. Hence, while mobile sensors can *augment* other authentication or key-generation processes, they rarely suffice as a standalone replacement for dedicated, cryptographically validated entropy sources.

Table 5: Top 10 best-performing sensor combinations (SHL; in bits).

Modality	H_0	H_1	H_2	H_∞
All sensors	158.601	82.301	39.320	21.289
(Acc.{x,y,z}, Gyro.{x,y,z}, Mag.{x,y,z}, Ori.{w,x,y,z}, Grav.{x,y,z}, LinAcc.{y,z}, Pres., Alt., Temp.)	148.995	78.624	39.276	21.289
(Acc.{x,y,z}, Gyro.{x,y,z}, Mag.{x,y,z}, Ori.{w,x,y,z}, Grav.{x,y,z}, LinAcc.{x,z}, Pres., Alt., Temp.)	148.759	78.477	39.272	21.289
(Acc.{x,y,z}, Gyro.{x,z}, Mag.{x,y,z}, Ori.{w,x,y,z}, Grav.{x,y,z}, LinAcc.{x,y,z}, Pres., Alt., Temp.)	148.587	78.380	39.249	21.289
(Acc.{x,y,z}, Gyro.{x,y,z}, Mag.{x,y,z}, Ori.{w,x,y,z}, Grav.{x,y,z}, LinAcc.{x,y}, Pres., Alt., Temp.)	148.952	78.135	39.235	21.289
(Acc.{x,y,z}, Gyro.{x,y,z}, Mag.{x,y,z}, Ori.{w,x,y,z}, Grav.{x,y,z}, LinAcc.{z}, Pres., Alt., Temp.)	139.153	74.800	39.175	21.289
(Acc.{x,y,z}, Gyro.{x,z}, Mag.{x,y,z}, Ori.{w,x,y,z}, Grav.{x,y,z}, LinAcc.{y,z}, Pres., Alt., Temp.)	138.981	74.703	39.128	21.289
(Acc.{x,y,z}, Gyro.{x,z}, Mag.{x,y,z}, Ori.{w,x,y,z}, Grav.{x,y,z}, LinAcc.{x,z}, Pres., Alt., Temp.)	138.745	74.556	39.117	21.289
(Acc.{x,y,z}, Gyro.{x,y,z}, Mag.{x,y,z}, Ori.{w,x,y,z}, Grav.{x,y,z}, LinAcc.{y}, Pres., Alt., Temp.)	139.346	74.458	39.100	21.289
(Acc.{x,y,z}, Gyro.{x,y,z}, Mag.{x,y,z}, Ori.{w,x,y,z}, Grav.{x,y,z}, LinAcc.{x}, Pres., Alt., Temp.)	139.109	74.311	39.087	21.289

Can Extractors Salvage Weak Sources? One might hope that cryptographic extractors (e.g. Von Neumann extractors or more advanced schemes [46–48]) could mitigate low-entropy sensor data. Indeed, extractors are designed to reduce bias in a noisy or skewed source. However, they cannot *increase* the total amount of randomness beyond the source’s intrinsic min-entropy. In other words, if the combined sensor data only provides around 24 bits of min-entropy, then post-processing can at best produce a short, unbiased bitstring reflecting those 24 bits, and no more. From a security standpoint, this means that an extractor can *improve the quality of the randomness* (i.e., make it more uniform) but not *increase the quantity* (i.e., its total brute-force resistance). Thus, while extraction can help if the original data has enough min-entropy to meet system requirements, it cannot elevate a weak source—one that fundamentally lacks sufficient min-entropy—to the higher security thresholds often demanded by rigorous standards.

5.2 Limitations

Despite our comprehensive multivariate analysis, this work has some limitations. Firstly, although we analyse four large datasets, they do not fully capture contexts all possible contexts. For example, work has suggested that performing dedicated movements (e.g. gestures) can increase the amount of usable entropy from motion sensors, on the order of magnitude of 5–6 bits [19, 25]. Our datasets

do not cover such dedicated movements; it is possible that the reported results are an underestimation of entropy for motion-based sensors. Secondly, our choice of Freedman-Diaconis binning and Chow-Liu trees is a pragmatic compromise. Smaller bin sizes tend to over-simplify the distribution and underestimate entropy, whereas larger bins can lead to computational blowup. Although our approach outperforms naive joint entropy estimation, it is still an approximation. Thirdly, we largely focus on a data-centric view of entropy and do not deeply explore sophisticated adversarial strategies, such as sensor spoofing [20], fault injection attacks [34] or cross-modality correlation attacks (e.g. see [49] for such attacks against wireless body area networks). These threats may significantly reduce the usable entropy of sensors even further.

6 Conclusion

This paper provides a comprehensive analysis of sensor-derived entropy across multiple datasets and modalities. Our results expose a tension between the *perceived* and *actual* strength of sensor data for security applications. Even in the best-performing sensor combinations, seemingly suitable results using one metric collapse to insecure levels when using standard worst-case metrics. Notably, modalities that yield ‘good’ max- or Shannon entropies, representing the best- and average-case unpredictability, have insecure worst-case min-entropies. Consequently, sensor modalities that may appear robust have biases that may enable adversaries to predict the most probable values with minimal effort.

Our findings also challenge the prevailing evaluation approach that machine learning metrics (e.g., accuracy or EER) suffice to demonstrate the inherent randomness of sensor signals. The vulnerability of mobile sensors to biased distributions significantly undermine their effectiveness as reliable entropy sources. We also cast doubt on the use of sensors with respect to their non-stationary and lack of reproducibility. These issues collectively contradict the criteria articulated in frameworks such as NIST SP 800-90B, which emphasise noise-source stationarity and protection from external influence. The effectiveness of countermeasures remains an open research challenge. Our hope is that the methodologies and insights presented here will encourage the security community to adopt more rigorous evaluation strategies for sensor-based techniques, and ultimately pave the way for safer and more robust designs in mobile-device security.

In future work, we consider that a dynamic analysis is important to assess the stationarity issues with sensor data, where entropy varies according to user behavior or environment. Moreover, a user study could yield empirical bounds on how finely humans can *intentionally* manipulate motion sensors, revealing more realistic limits to sensor-based randomness in real-world scenarios. For example, our binning decision was a statistical one, rather one that reflects human usage; it is possible that real-world usage may reduce the resolution of useful sensor data, thus reducing entropy. Overall, while sensor-based data can reach limited levels of entropy under favourable conditions, the road to making such sources systematically *secure* and *robust* is long. The key takeaway is that researchers

and engineers should resist the temptation to treat sensor readings as *bona fide* random bits. Substantial work is needed before sensors can be considered as appropriate sources of randomness for security-critical applications.

Acknowledgments Carlton Shepherd has received funding from the UK EP-SRC ‘Chameleon’ project (EP/Y030168/1). The authors would like to thank Darren Hurley-Smith for insightful conversations on the topic.

References

1. R. Mayrhofer and H. Gellersen, “Shake well before use: Intuitive and secure pairing of mobile devices,” *IEEE Transactions on Mobile Computing*, 2009.
2. B. Shrestha, N. Saxena, H. T. T. Truong, and N. Asokan, “Drone to the rescue: Relay-resilient authentication using ambient multi-sensing,” in *International Conference on Financial Cryptography and Data Security*, pp. 349–364, Springer, 2014.
3. J. Krhovják, P. Švenda, V. Matyáš, *et al.*, “The sources of randomness in mobile devices,” in *Proceedings of 12th Nordic Conference on Secure IT Systems*, 2007.
4. K. Markantonakis, J. A. Meister, I. Gurulian, C. Shepherd, R. N. Akram, S. A. Ghazalah, M. Kasi, D. Sauveron, and G. Hancke, “Using ambient sensors for proximity and relay attack detection in NFC transactions: A reproducibility study,” *IEEE Access*, 2024.
5. H. T. T. Truong, X. Gao, B. Shrestha, N. Saxena, N. Asokan, and P. Nurmi, “Comparing and fusing different sensor modalities for relay attack resistance in zero-interaction authentication,” in *IEEE Int’l Conf. on Pervasive Computing and Communications*, IEEE, 2014.
6. M. Mehrnezhad, F. Hao, and S. F. Shahandashti, “Tap-tap and pay (TTP): Preventing the mafia attack in nfc payment,” in *Proceedings of the 2nd International Conference on Security Standardisation Research*, SSR, pp. 21–39, Springer, 2015.
7. I. Gurulian, K. Markantonakis, E. Frank, and R. N. Akram, “Good vibrations: artificial ambience-based relay attack detection,” in *17th IEEE Int’l Conf. on Trust, Security and Privacy In Computing and Communications*, IEEE, 2018.
8. T. Halevi, D. Ma, N. Saxena, and T. Xiang, “Secure proximity detection for NFC devices based on ambient sensor data,” in *17th European Symposium on Research in Computer Security*, ESORICS, pp. 379–396, Springer, 2012.
9. V. M. Patel, R. Chellappa, D. Chandra, and B. Barbello, “Continuous user authentication on mobile devices: Recent progress and remaining challenges,” *IEEE Signal Processing Magazine*, vol. 33, no. 4, pp. 49–61, 2016.
10. S. Mekruksavanich and A. Jitpattanakul, “Deep learning approaches for continuous authentication based on activity patterns using mobile sensing,” *Sensors*, 2021.
11. E. Hayashi, S. Das, S. Amini, J. Hong, and I. Oakley, “CASA: Context-aware scalable authentication,” in *9th Symposium on Usable Privacy and Security*, 2013.
12. O. Riva, C. Qin, K. Strauss, and D. Lymberopoulos, “Progressive authentication: deciding when to authenticate on mobile phones,” in *21st USENIX Security Symposium*, pp. 301–316, 2012.
13. W. Shi, J. Yang, Y. Jiang, F. Yang, and Y. Xiong, “Senguard: Passive user identification on smartphones using multiple sensors,” in *7th Int’l Conf. on Wireless and Mobile Computing, Networking and Communications*, IEEE, 2011.

14. N. Micallef, M. Just, L. Baillie, M. Halvey, and H. G. Kayacik, "Why aren't users using protection? investigating the usability of smartphone locking," in *17th Int'l Conf. on Human-Computer Interaction with Mobile Devices and Services*, 2015.
15. M. Miettinen, S. Heuser, W. Kronz, A.-R. Sadeghi, and N. Asokan, "Conxsense: automated context classification for context-aware access control," in *9th ACM Symposium on Information, Computer and Communications Security*, 2014.
16. L. Li, X. Zhao, and G. Xue, "Unobservable re-authentication for smartphones.," in *Network and Distributed System Security*, Citeseer, 2013.
17. S. Pan, C. Ruiz, J. Han, A. Bannis, P. Tague, H. Y. Noh, and P. Zhang, "Universense: IoT device pairing through heterogeneous sensing signals," in *19th Int'l Workshop on Mobile Computing Systems and Applications*, 2018.
18. S. Uellenbeck, M. Dürmuth, C. Wolf, and T. Holz, "Quantifying the security of graphical passwords: The case of android unlock patterns," in *ACM SIGSAC Conf. on Computer and Communications Security*, 2013.
19. J. Voris, N. Saxena, and T. Halevi, "Accelerometers and randomness: Perfect together," in *4th ACM Conf. on Wireless Network Security*, 2011.
20. B. Shrestha, N. Saxena, H. T. T. Truong, and N. Asokan, "Sensor-based proximity detection in the face of active adversaries," *IEEE Transactions on Mobile Computing*, vol. 18, no. 2, pp. 444–457, 2018.
21. X. Li, Q. Zeng, L. Luo, and T. Luo, "T2pair: Secure and usable pairing for heterogeneous IoT devices," in *ACM Computer and Communications Security*, 2020.
22. C. Wu, X. Li, L. Luo, and Q. Zeng, "T2Pair++: Secure and usable IoT pairing with zero information loss," *arXiv preprint arXiv:2409.16530*, 2024.
23. I. Gurulian, C. Shepherd, E. Frank, K. Markantonakis, R. Akram, and K. Mayes, "On the effectiveness of ambient sensing for NFC-based proximity detection by applying relay attack data," in *16th IEEE International Conference on Trust, Security and Privacy in Computing and Communications*, vol. 17, 2017.
24. C. Shepherd, I. Gurulian, E. Frank, K. Markantonakis, R. N. Akram, E. Panaousis, and K. Mayes, "The applicability of ambient sensors as proximity evidence for NFC transactions," in *IEEE Security and Privacy Workshops*, pp. 179–188, IEEE, 2017.
25. N. Lv, T. Chen, and Y. Ma, "Analysis on entropy sources based on smartphone sensors," in *10th Int'l Conf. on Communication and Network Security*, 2020.
26. C. Hennebert, H. Hossayni, and C. Lauradoux, "Entropy harvesting from physical sensors," in *6th ACM Security and Privacy in Wireless and Mobile Networks*, 2013.
27. A. Suci, D. Lebu, and K. Marton, "Unpredictable random number generator based on mobile sensors," in *IEEE 7th Int'l Conference on intelligent Computer Communication and Processing*, pp. 445–448, IEEE, 2011.
28. A. Rukhin, J. Soto, J. Nechvatal, M. Smid, E. Barker, S. Leigh, M. Levenson, M. Vangel, D. Banks, N. Heckert, J. Dray, and S. Vo, "A Statistical Test Suite for Random and Pseudorandom Number Generators for Cryptographic Applications," Tech. Rep. SP 800-22, National Institute of Standards and Technology, April 2001.
29. K. Wallace, K. Moran, E. Novak, G. Zhou, and K. Sun, "Toward sensor-based random number generation for mobile and IoT devices," *IEEE Internet of Things Journal*, vol. 3, no. 6, pp. 1189–1201, 2016.
30. D. Hurley-Smith and J. Hernandez-Castro, "Quantum leap and crash: Searching and finding bias in quantum random number generators," *ACM Transactions on Privacy and Security*, vol. 23, no. 3, pp. 1–25, 2020.
31. G. Mai, M.-H. Lim, and P. C. Yuen, "On the guessability of binary biometric templates: A practical guessing entropy based approach," in *IEEE Int'l Joint Conf. on Biometrics*, IEEE, 2017.

32. M. S. Turan, E. Barker, J. Kelsey, K. A. McKay, M. L. Baish, M. Boyle, *et al.*, “Recommendation for the entropy sources used for random bit generation,” *NIST Special Publication*, vol. 800, no. 90B, p. 102, 2018.
33. Bundesamt für Sicherheit in der Informationstechnik (BSI), “A Proposal for Functionality Classes for Random Number Generators (Version 3.0),” tech. rep., Federal Office for Information Security (BSI), September 2024.
34. C. Shepherd, K. Markantonakis, N. van Heijningen, D. Aboukassimi, C. Gaine, T. Heckmann, and D. Naccache, “Physical fault injection and side-channel attacks on mobile devices: A comprehensive analysis,” *Computers & Security*, 2021.
35. D. Buller and A. Kaufer, “Estimating min-entropy using probabilistic graphical models,” in *Random Bit Generation Workshop*, NIST, 2016.
36. U. Mahbub, S. Sarkar, V. M. Patel, and R. Chellappa, “Active user authentication for smartphones: A challenge data set and benchmark results,” in *IEEE 8th Int’l Conf. on Biometrics Theory, Applications and Systems*, Sept 2016.
37. G. Stragapede, R. Vera-Rodriguez, R. Tolosana, and A. Morales, “BehavePassDB: public database for mobile behavioral biometrics and benchmark evaluation,” *Pattern Recognition*, vol. 134, p. 109089, 2023.
38. A. Acién, A. Morales, J. Fierrez, R. Vera-Rodriguez, and O. Delgado-Mohatar, “Be-CAPTCHA: Behavioral bot detection using touchscreen and mobile sensors benchmarked on HuMIdb,” *Engineering Applications of Artificial Intelligence*, 2021.
39. D. Anguita, A. Ghio, L. Oneto, X. Parra, J. L. Reyes-Ortiz, *et al.*, “A public domain dataset for human activity recognition using smartphones,” in *Esann*, 2013.
40. H. Gjoreski, M. Ciliberto, L. Wang, F. J. O. Morales, S. Mekki, S. Valentin, and D. Roggen, “University of Sussex–Huawei locomotion and transportation dataset for multimodal analytics with mobile devices,” *IEEE Access*, 2018.
41. L. Wang, H. Gjoreski, M. Ciliberto, S. Mekki, S. Valentin, and D. Roggen, “Enabling reproducible research in sensor-based transportation mode recognition with the Sussex–Huawei dataset,” *IEEE Access*, vol. 7, pp. 10870–10891, 2019.
42. M. Fomichev, M. Maass, L. Almon, A. Molina, and M. Hollick, “Perils of zero-interaction security in the Internet of Things,” *Proc. ACM on Interactive, Mobile, Wearable and Ubiquitous Technologies*, vol. 3, no. 1, pp. 1–38, 2019.
43. “Bosch BMA400 accelerometer.” <https://www.bosch-sensortec.com/products/motion-sensors/accelerometers/bma400/>, 2025. Accessed: 12 Feb 2025.
44. C. Chow and C. Liu, “Approximating discrete probability distributions with dependence trees,” *IEEE Trans. on Information Theory*, vol. 14, no. 3, 1968.
45. A. Ankan and J. Textor, “pgmpy: A Python toolkit for Bayesian networks,” *Journal of Machine Learning Research*, vol. 25, no. 265, pp. 1–8, 2024.
46. J. Von Neumann, “Various techniques used in connection with random digits,” *Applied Math Series*, vol. 12, no. 36-38, p. 5, 1951.
47. L. Trevisan *et al.*, “Extractors and pseudorandom generators,” *Journal of the ACM*, vol. 48, no. 4, pp. 860–879, 2001.
48. B. Barak, R. Shaltiel, and E. Tromer, “True random number generators secure in a changing environment,” in *Cryptographic Hardware and Embedded Systems*, pp. 166–180, Springer, 2003.
49. R. Dautov and G. R. Tsouri, “Effects of passive negative correlation attack on sensors utilizing physical key extraction in indoor wireless body area networks,” *IEEE Sensors Letters*, vol. 3, no. 7, pp. 1–4, 2019.